JOTCS A
Journal of the Turkish Chemical Society
Section: A
Chemistry
TURKISH CHEMICAL SOCIETY

LDH- ɣ-Fe_2O_3-MoS_2 Composite for Vegetable Oil and Pb^{2+} Removal From Water

Fatih Mehmet EMEN[1], Ruken Esra DEMİRDÖĞEN[2], Göktürk AVSAR[3], Ali İhsan KARAÇOLAK[1]

[1]Mehmet Akif Ersoy University, Faculty of Arts and Science, Department of Chemistry, TR 15030, Burdur, Turkey
[2]Çankiri Karatekin University, Faculty of Science Department of Chemistry, TR 18100, Çankırı, Turkey
[3]Mersin University, Faculty of Arts and Science, Department of Chemistry, TR 15030, Burdur, Turkey

Abstract: Water pollution is a global concern. Inorganic and organic pollutants constitute primary pollutants in water resources. Therefore, it is of great concern to develop advanced sorbent materials for effective and efficient removal of metals and oil from water. In this study, synthesis of new LDH composites which would be used for sorption of heavy metals and oils from polluted water. For this purpose, MgAlOH-ɣ-Fe_2O_3-MoS_2 composite was prepared and characterizations were performed by FT-IR and XRD. The XRD powder pattern of the composite showed that it contained γ-Fe_2O_3, $MgAl(OH)14.xH_2O$ and MoS_2. Thermal stability of the composite was investigated via DTA/TG technique. MgAlOH-ɣ-Fe_2O_3-MoS_2 composite showed highly efficient sorption for vegetable oil up to 418% times of its own weight. The ability of MgAlOH- ɣ-Fe_2O_3-MoS_2 composite for removing Pb^{2+} ions from aqueous solution. Pb^{2+} ion analysis was made by ICP-OES. The effect of Pb^{2+} amounts, pH, sorbent amounts, and solvent flow rate on the adsorption capacity of MgAlOH- ɣ-Fe_2O_3-MoS_2 composite were also investigated.

Keywords: ɣ-Fe_2O_3, nanoparticle, composite, MoS_2, LDH.

Submitted: October 02, 2018. **Accepted:** January 18, 2019.

Cite this: Emen F, Demirdöğen R, Avşar G, Karaçolak A. LDH- ɣ-Fe2O3-MoS2 Composite for Vegetable Oil and Pb2+ Removal From Water. Journal of the Turkish Chemical Society, Section A: Chemistry. 2019;6(1):35–40.

DOI: https://dx.doi.org/10.18596/jotcsa.466768.

***Corresponding author.** E-mail: femen106@gmail.com, Tel: +905077681688, Fax:+902482133099.

INTRODUCTION

Water pollution is a global problem. Inorganic and organic pollutants are known as primary pollutants in water resources. Therefore, for eco-efficient and effective removal of metal ions and oil from water advanced sorbent materials should be developed (1). The photocatalytic deterioration which is the solution of environmental problems arising from organic pollutants, has attracted the attention of many researchers in recent years (2). A wide range of synthetic materials have been proposed and applied for this purpose (3–9). Due to its suitable physicochemical and optical properties, TiO_2, ZnO, Fe_2O_3, etc. metal oxide nanoparticles are promising candidates for photocatalytic applications (5,3–9). Molybdenum disulfide (MoS_2) has been widely used in biomedical applications as it has excellent photothermal conversion ability. Transition metal dichalogenes (TMDCs) are a family of two-dimensional layered materials with interesting physical, electronic, and chemical properties (10). The atoms in the layers are held together by strong covalent interactions and the layers are deposited along the van der Waals forces (11, 12). TMDCs have been extensively studied in energy storage, sensors, catalysis and biomedical (13-17). In particular, MoS_2, WS_2 and WSe_2 can be used in a wide variety of biomedical applications because their chalcogenides are less toxic than graphene (18). Oil pollution causing by oil spills has been an environmental and ecological disaster. The oil

spill in the Gulf of Mexico and the Bohai Gulf of China have shown the difficulty of an effective oil spill clearance. Mechanical extraction with sorbents is considered to be one of the most economical and efficient methods (19). In this process, the preparation of efficient, cost-effective materials for oil-water separation has gained importance. To date, different materials such as natural absorbers, microporous polymers, expanded graphite, carbon nanotubes and nanowire membranes have been used for this purpose (20). However, having several disadvantages, such as low oil loading capacity, excessive cost or environmental and ecological risk, limit the extensive application of these materials.

In this study, MgAlOH- ɣ-Fe_2O_3-MoS_2 composite was prepared and characterized via FT-IR and XRD techniques. The sorption studies of Pb^{2+} ion and vegetable oil from polluted water was carried out.

Herein, lightweight, hydrophobic, and porous aerogels made of carbon microbelts (CMBs) are first produced via a facile route by using waste paper as the raw material. Importantly, the CMB aerogel can absorb a wide range of organic compounds.

MATERIALS AND METHODS

Synthesis of Compounds

Synthesis of MCM-41

Typically, 0.6 g of n-cetyltrimethylammonium bromide (CTAB) was first dissolved in 400 mL of deionized water. Then 3.5 mL of 2 mol/L NaOH was added to the solution, followed by adjusting the solution temperature to 80 °C. Subsequently, 2.5 mL of TEOS was added dropwise to above solution with vigorous stirring. The mixture was stirred for another 2 h to give rise to a white solid. The obtained solid product was filtered, washed with deionized water and ethanol, and then dried in air. The dried sample was calcined at 550 °C for 1 h in N_2 and followed by another 3 h in air to remove the organic template.

Sythesis of mesoporous ɣ-Fe_2O_3

$Fe(NO_3)_3$ was dissolved in ethanol and MCM-41 was added to solution and stirred for 2 h. After the fitration, the powder was dried at 100 °C and fired at 550 °C for 3 h. The obtained MCM-41-Fe_2O_3 was added to 10 M NaOH and heated to dissolve MCM-41 phase. The obtained mesoporous Fe_2O_3 was washed and dried.

Preparation of MgAlOH-ɣ-Fe_2O_3-MoS_2

A portion of 50 mL of an aqueous solution containing 56.07 mmol (11.4 g) $MgCl_2$ $6H_2O$ and 28.17 mmol (6.8 g) $AlCl_3$ $6H_2O$ was added to 75 mL of an aqueous solution containing 12.52 mmol (2 g) Fe_2O_3 and $1{,}25x10^{-5}$ mmol (2 g) MoS_2 (12.50 mmol) The pH was raised to a value of 9 by addition of 2 M NaOH and the mixture was sonicated at room temperature for 16 h. The solid was filtered, washed, and dried in a vacuum desiccator.

Characterization

X-ray diffraction pattern was recorded on Bruker D8 using Cu Kα radiation, with the diffraction angle (2Θ) at a range of 10–80◦. FT-IR spectrum was recorded on a Perkin Elmer FT-IR/FIR/NIR spectrometer Frontier ATR system. Thermal stability of the composite was investigated via DTA/TG technique. Heavy metal analysis was made by ICP-OES. Measurements were carried out with a sequential, axially viewed Perkin Elmer Optima 8000 ICP-OES equipped with a meinhard nebulizer, a glass cyclonic spray chamber and ICP WinLab software Data System. Optimized operating conditions for the determination of constituents in water by ICP OES are given in Table 1.

Table 1. Optimized operating conditions for the determination of constituents in water by ICP OES

Rf power (W)	1450
Injector:	Alumina 2 mm i.d.
Sample tubing:	Standard 0.76 mm i.d
Drain tubing:	Standard 1.14 mm i.d.
Quartz torch:	Single slot
Sample capillary:	PTFE 1 mm i.d.
Sample vials:	Polypropylene
Source equilibrium delay:	15 sec
Plasma viewing:	Axial
Processing mode:	Peak area
Gases:	Argon and Nitrogen
Shear Gas:	Air

Sorption of Vegetable Oil

In a typical sorption test, MgAlOH-Fe_2O_3-MoS_2 composite was placed in contact with a vegetable oil emulsion in water until the composite was filled with the oil, which was then taken out for weight measurement. The weight measurement should be done quickly. The weight of a piece of the composite before and after sorption was recorded for calculation of the weight gain.

RESULTS AND DISCUSSION

FT-IR studies of MgAlOH-ɣ-Fe_2O_3-MoS_2

FT-IR spectrum of the MgAlOH-ɣ-Fe_2O_3-MoS_2 is given in Figure 1. Asymmetric vibration band of the O-H group of MgAlOH is observed at 3356 cm^{-1}. FT-IR spectrum of Fe_2O_3 exhibited vibrations in the region of 400-600 cm^{-1} which can be attributed to the vibrations of Fe-O and Mo-S (443 cm^{-1}) which confirms Fe_2O_3 nanoparticles and MoS_2 sheet structure. The results indicate the accuracy of the proposed structure (21-23).

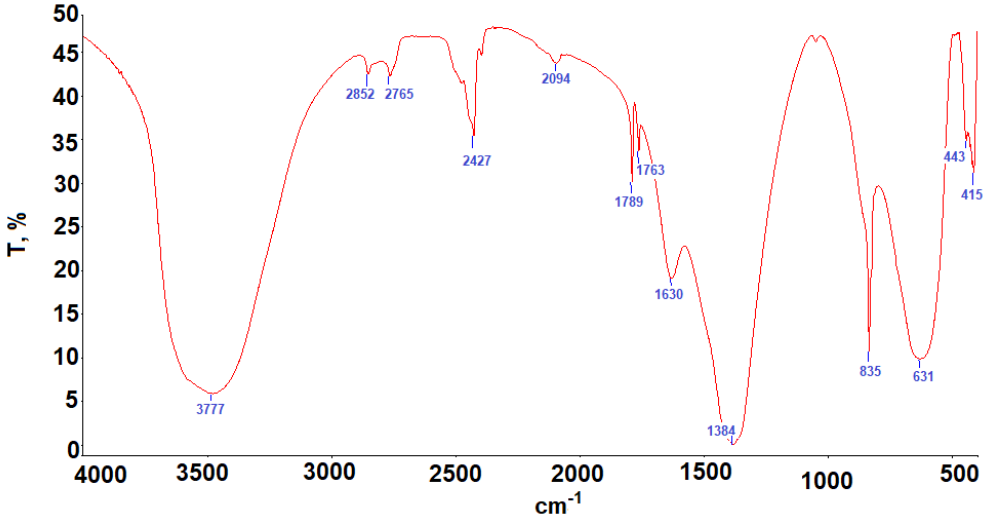

Figure 1: FT-IR spectrum of MgAlOH-Fe_2O_3-MoS_2.

XRD studies of MgAlOH-ɣ-Fe_2O_3-MoS_2

XRD powder diffraction pattern of MgAlOH-ɣ-Fe_2O_3-MoS_2 is presented in Figure 2. The XRD powder pattern of the composite showed that it contained γ-Fe_2O_3 (PDF card no:00-002-1047), $MgAl(OH)_{14}.XH_2O$ (PDF card no:00-043-0072) and MoS_2 (PDF card no:00-037-4492).

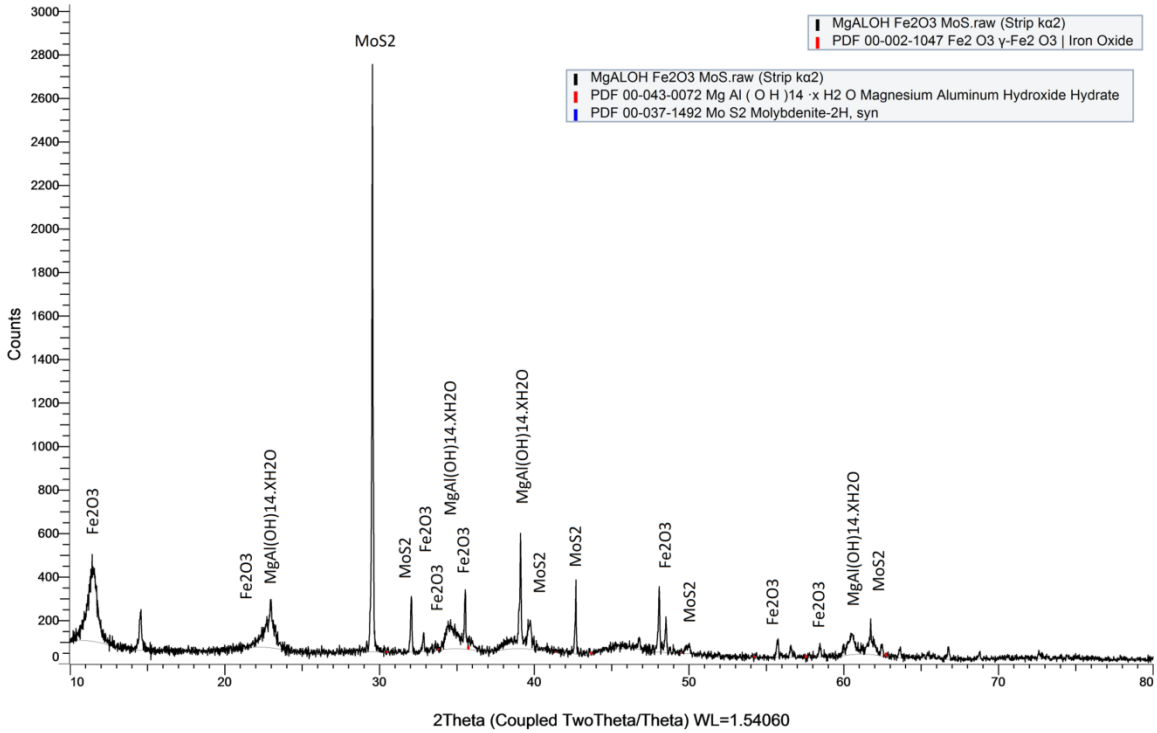

Figure 2: XRD powder diffraction pattern of MgAlOH-ɣ-Fe_2O_3-MoS_2

Thermal Analysis of MgAlOH-ɣ-Fe_2O_3-MoS_2

TG/DTA/DTG curves of MgAlOH-ɣ-Fe_2O_3-MoS_2 are given in Figure 3. In TG and DTG curves, three decomposition stages were obtained between 30 °C and 700 °C for MgAlOH-Fe_2O_3-MoS_2 . These decompositions were attributed to MgAlOH. The remaining products are MgO, Al_2O_3, Fe_2O_3 and MoS_2 mixture. Three endothermic peaks of decomposition stages were observed at 50 °C, 300 °C and 670 °C, respectively.

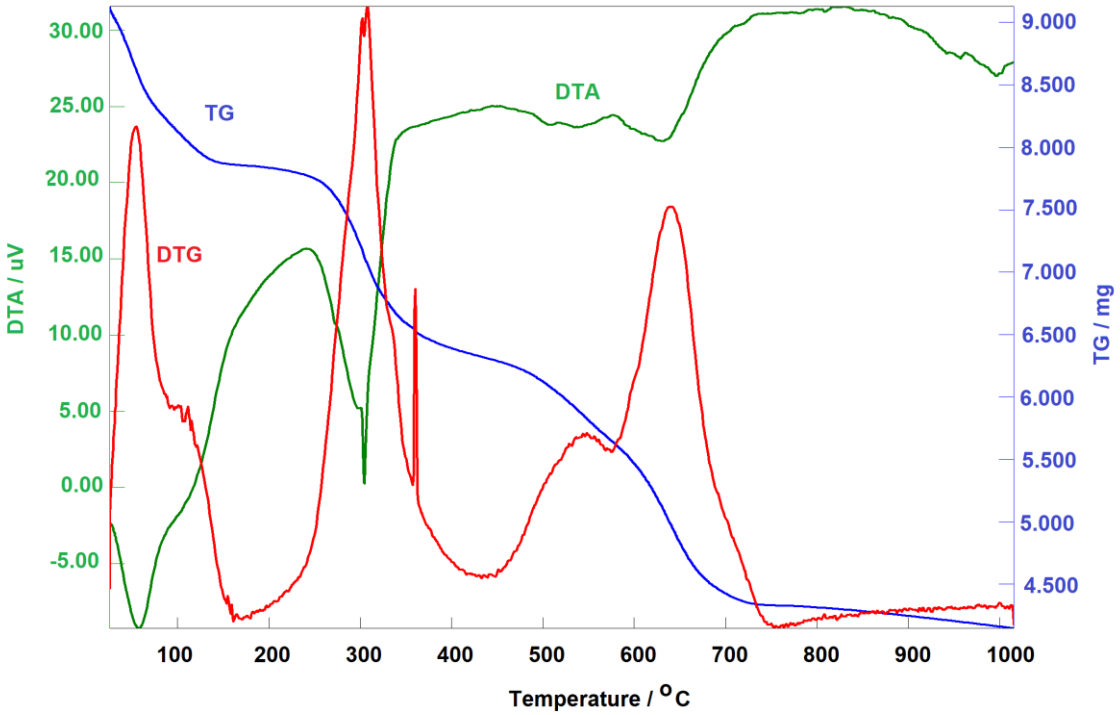

Figure 3: TG/DTA/DTG curves of MgAlOH-Fe_2O_3-MoS_2.

Absorption studies

Lead ion solutions of various volumes ranging from 1.1 mL to 4.2 mL, depending on the concentration of the lead ions in the solution, were passed through the column. The sorbed Pb^{2+} ions were eluted with 0.01 M hot nitric acid solution. Lead determination was made by ICP-OES at 217.0 nm and limit of detection was 0.1 mg/L. Effect of pH and concentration of Pb^{2+} as well as maximum sorption capacity was determined.

The obtained results are given in Tables 2-5.

Table 2. pH effect on adsorption capacity of MgAlOH-ɣ-Fe_2O_3-MoS_2.

MgAlOH-ɣ-Fe_2O_3-MoS_2	Pb concentration in solution	Adsorption	Recovery (%)
pH=3	420 ppm	403.3 ppm	96
pH=6	420 ppm	412.07 ppm	98
pH=7	420 ppm	415.93 ppm	99

Table 3. The effect of Pb^{2+} amounts on adsorption capacity of MgAlOH-ɣ-Fe_2O_3-MoS_2

Pb concentration in solution	Adsorption	Recovery (%)
420 ppm	415.07 ppm	98.1
320 ppm	312,94 ppm	97.6
215 ppm	212.1 ppm	98.2

Table 4. The effect of sorbent amounts on adsorption capacity of MgAlOH-ɣ-Fe_2O_3-MoS_2

Amount of MgAlOH-ɣ-Fe_2O_3-MoS_2	Pb concentration in solution	Adsorption	Recovery (%)
0.2 g	420 ppm	415 ppm	99.2
0.3 g	420 ppm	-	100

Table 5. The effect of solvent flow rate on adsorption capacity of MgAlOH-ɣ-Fe_2O_3-MoS_2

Solvent flow rate	Pb concentration in solution	Adsorption	Recovery (%)
1.1 mL/dk	420 ppm	416.7 ppm	99.4
2.7 mL/dk	420 ppm	413 ppm	98.1
4.2 mL/dk	420 ppm	405 ppm	96

Oil Sorption studies

0.5 g MgAlOH-ɣ-Fe_2O_3-MoS_2 was weighed and added onto water/oil (30 mL/4 mL) and sonicated for 30 min. Then the sorbent material was decanted and dried at 100 °C for 2 h. 0.5 g MgAlOH-ɣ-Fe_2O_3-MoS_2 absorbed 2.05 g oil. These result revealed that oil sorption capacity of MgAlOH-ɣ-Fe_2O_3-MoS_2 is 418%. The images MgAlOH-ɣ-Fe_2O_3-MoS_2 and oil adsorbed MgAlOH-ɣ-Fe_2O_3-MoS_2 are shown in Figure 4.

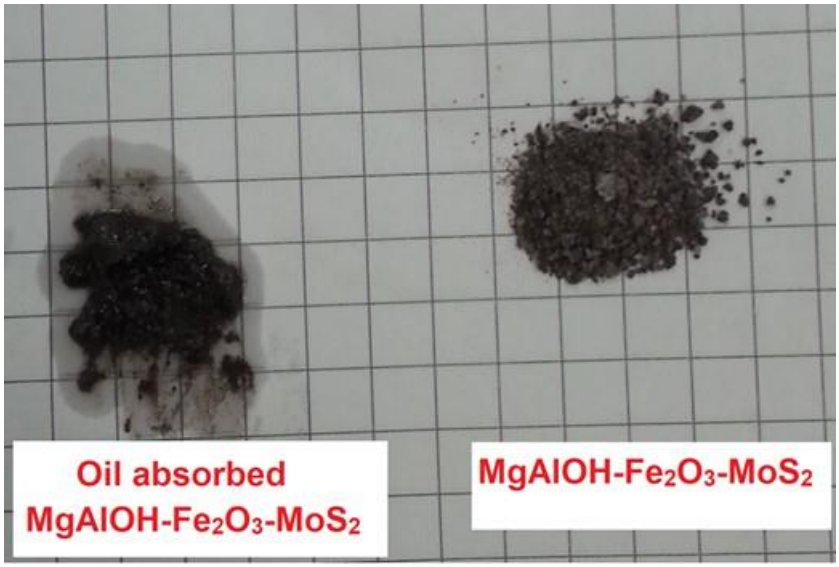

Figure 4. The images of MgAlOH-ɣ-Fe_2O_3-MoS_2 and oil-adsorbed MgAlOH-ɣ-Fe_2O_3-MoS_2.

CONCLUSION

In this study, MgAlOH-ɣ-Fe_2O_3-MoS_2 composite was prepared. The structure of MgAlOH-ɣ-Fe_2O_3-MoS_2 was elucidated by FT-IR and XRD powder pattern methods. The XRD powder pattern of the composite showed that it contained γ-Fe_2O_3, $MgAl(OH)14.xH_2O$ and MoS_2. The thermal behavior of the composite was investigated by DTA/TG combined system. In TG curves, three decomposition stages were obtained between 30 °C and 700 °C for MgAlOH-ɣ-Fe_2O_3-MoS_2. Double layer hydroxides are composed of layers. LDHs have the ability to absorb various cations and anions between layers. In recent years, magnetic nanoadsorbents and magnetic composites (24) have been widely used in the removal of heavy metals, various anions, organic pollutants and dyestuffs from solution media, for the removal of water as well as used in the recovery of these adsorbents and their evaluation after regeneration Furthermore, magnetic nanoadsorbents and magnetic composites (24) have been used for the removal of heavy metals, various anions, organic pollutants and dyestuffs from solution media. Recovering of these adsorbents and evaluation after regeneration are widely studied (25). Fe_2O_3 with the magnetic properties are known to absorb some heavy metal ions. It is also used to remove MoS_2 oils from the water. MgAlOH-ɣ-Fe_2O_3-MoS_2 composite can be used not only to remove heavy metals from contaminated water but also to remove oils. The results revealed that MgAlOH-ɣ-Fe_2O_3-MoS_2 composite was shown highly efficient sorption for vegetable oil up to 418% times weight itself.

REFERENCES

1. Gao X, Wang X, Ouyang X, Wen C. Flexible Superhydrophobic and Superoleophilic MoS_2 Sponge for Highly Efficient Oil-Water Separation. Sci. Rep-UK. 2016; 6:27207.

2. Karimi M, Jahangir V, Ezzati M, Saydi J, Lejbini MB. Zn0. 94Cd0. 06O nanoparticles with various structures, morphologies and optical properties toward MB optodecolorization. Opt. Mater. 2014; 36(3):697-703.

3. Putri LK, Tan LL, Ong WJ, Chang WS, Chai SP. Graphene oxide: exploiting its unique properties toward visible-light-driven photocatalysis. Appl.Mater. Today. 2016; 4:9-16.

4. Li M, Huang H, Yu S, Tian N, Dong F, Du X, Zhang Y. Simultaneously promoting charge separation and photoabsorption of BiOX (X= Cl, Br) for efficient visible-light photocatalysis and photosensitization by compositing low-cost biochar. Appl. Surf. Sci. 2016; 386:285-95.

5. Mazhdi M, Saydi J, Karimi M, Seidi J, Mazhdi F. A study on optical, photoluminescence and thermoluminescence properties of ZnO and Mn doped-ZnO nanocrystalline particles. Optik 2013; 124(20):4128-33.

6. Askari MB, Banizi ZT, Soltani S, Seifi M. Comparison of optical properties and photocatalytic behavior of TiO2/MWCNT, CdS/MWCNT and TiO2/CdS/MWCNT nanocomposites. Optik. 2018; 157:230-9.

7. Bystrov VS, Piccirillo C, Tobaldi DM, Castro, PML, Coutinho J, Kopyl S, Pullar RC. Oxygen vacancies, the optical band gap (Eg) and photocatalysis of hydroxyapatite: comparing modelling with measured data. Appl. Catal. B: Environ. 2016; 196:100-7.

8. Güler SH, Güler Ö, Evin E, Islak S. Electrical and optical properties of ZnO-milled Fe2O3 nanocomposites produced by powder metallurgy route. Optik. 2016; 127(6):3187-91.

9. Yin Q, Qiao R, Zhu L, Li Z, Li M, Wu W. α-Fe2O3 decorated ZnO nanorod-assembled hollow microspheres: Synthesis and enhanced visible-light photocatalysis. Mater. Lett. 2014; 135:135-8.

10. Wang QH, Kalantar-Zadeh K, Kis A, Coleman JN, Strano MS. Electronics and optoelectronics of two-dimensional transition metal dichalcogenides. Nat. Nanotechnol. 2012; 7(11):699.

11. Chhowalla M, Shin HS, Eda G, Li, LJ Loh, KP, Zhang H. The chemistry of two-dimensional layered transition metal dichalcogenide nanosheets. Nat. Chem. 2013; 5(4):263.

12. Voiry D, Mohite A, Chhowalla M. Phase engineering of transition metal dichalcogenides. Chem. Soc. Rev. 2015; 44(9):2702-12.

13. Kalantar-zadeh K, Ou JZ, Daeneke T, Strano MS, Pumera M, Gras SL. (2015). Two-dimensional transition metal dichalcogenides in biosystems. Adv. Funct. Mater. 2015; 25(32):5086-99.

14. Yin W, Dong X, Yu J, Pan J, Yao Z, Gu Z, Zhao Y. MoS2-Nanosheet-Assisted Coordination of Metal Ions with Porphyrin for Rapid Detection and Removal of Cadmium Ions in Aqueous Media. ACS Appl. Mater. Inter. 2017; 9(25):21362-70.

15. Chen Y, Wu Y, Sun B, Liu S, Liu H. (2017). Two-Dimensional Nanomaterials for Cancer Nanotheranostics. Small. 2017; 13(10):1603446.

16. Song JX, Tang XY, Zhou DM, Zhang W, James TD, He XP, Tian H. A fluorogenic 2D glycosheet for the simultaneous identification of human-and avian-receptor specificity in influenza viruses. Mater. Horiz. 2017; 4(3):431-6.

17. Wahiba M, Feng XQ, Zang Y, James TD, Li J, Chen GR, He XP. A supramolecular pyrenyl glycoside-coated 2D MoS 2 composite electrode for selective cell capture. Chem. Commun. 2016; 52(78):11689-92.

18. Teo WZ, Chng ELK, Sofer Z, Pumera M. Cytotoxicity of Exfoliated Transition-Metal Dichalcogenides (MoS2, WS2, and WSe2) is Lower Than That of Graphene and its Analogues. Chemistry. 2014; 20(31):9627-32.

19. Zhu H, Qiu S, Jiang W, Wu D, Zhang C. Evaluation of electrospun polyvinyl chloride/polystyrene fibers as sorbent materials for oil spill cleanup. Environ. Sci. Technol. 2011; 45(10):4527-31.

20. Yuan J, Liu X, Akbulut O, Hu J, Suib SL, Kong J, Stellacci F. Superwetting nanowire membranes for selective absorption. Nat. Nanotechnol. 2008; 3(6):332.

21. Zhang H, Duan X, Ding Y. Preparation and investigation on a novel nanostructured magnetic base catalyst MgAl–OH-LDH/$CoFe_2O_4$, Mater. Chem. Phys. 2009;114(2-3): 795-801.

22. Willis AL. Turro NJ, O'Brien S. Spectroscopic Characterization of the Surface of Iron Oxide Nanocrystals, Chem. Mater. 2005;17:5970-5.

23. Wang H, Chen P, Wen F, Zhu Y, Zhang Y, Flower-like Fe_2O_3@MoS_2 nanocomposite decorated glassy carbon electrode for the determination of nitrite, Sens. Actuators B. 2015;220:749–54.

24. Sivashankar R, Sathya AB, Vasantharaj K, Sivasubramanian V. Magnetic composite an environmental super adsorbent for dye sequestration – A review. Environ. Nanotechnol.Monit. Manage. 2014, 1–2, 36–49.

25. Gómez-Pastora J, Bringas E, Ortiz I. Recent progress and future challenges on the use of high performance magnetic nano-adsorbents in environmental applications. Chem. Eng. J. 2014, 256, 187–204.